Title

Synthesis of linear and cyclic peptide-PEG-lipids for stabilization and targeting of cationic liposome-DNA complexes.

Authors

Ewert, Kai K
Kotamraju, Venkata Ramana
Majzoub, Ramsey N
et al.

Peer reviewed

Synthesis of Linear and Cyclic Peptide-PEG-Lipids for Stabilization and Targeting of Cationic Liposome–DNA Complexes

Kai K. Ewert[a,*], **Venkata Ramana Kotamraju**[b], **Ramsey N. Majzoub**[a,1], **Victoria M. Steffes**[a,c], **Emily A. Wonder**[a], **Tambet Teesalu**[b,d,e], **Erkki Ruoslahti**[b,e], and **Cyrus R. Safinya**[a,*]

[a]Department of Materials, Department of Physics and Department of Molecular, Cellular, and Developmental Biology, University of California, Santa Barbara, California 93106, United States

[b]Cancer Research Center, Sanford Burnham Prebys Medical Discovery Institute, La Jolla, California 92037, United States

[c]Department of Chemistry, University of California, Santa Barbara, California 93106, United States

[d]Center for Nanomedicine and Department of Molecular, Cellular, and Developmental Biology, University of California, Santa Barbara, California 93106, United States

[e]Laboratory of Cancer Biology, Institute of Biomedicine and Translational Medicine, University of Tartu, Tartu 50411, Estonia

Abstract

Because nucleic acids (NAs[2]) have immense potential value as therapeutics, the development of safe and effective synthetic NA vectors continues to attract much attention. *In vivo* applications of NA vectors require stabilized, nanometer-scale particles, but the commonly used approaches of steric stabilization with a polymer coat (e.g., PEGylation; PEG=poly(ethylene glycol)) interfere with attachment to cells, uptake, and endosomal escape. Conjugation of peptides to PEG-lipids can improve cell attachment and uptake for cationic liposome–DNA (CL–DNA) complexes. We present several synthetic approaches to peptide-PEG-lipids and discuss their merits and drawbacks. A lipid-PEG-amine building block served as the common key intermediate in all synthetic routes. Assembling the entire peptide-PEG-lipid by manual solid phase peptide synthesis (employing a lipid-PEG-carboxylic acid) allowed gram-scale synthesis but is mostly applicable to linear peptides connected via their N-terminus. Conjugation via thiol-maleimide or strain-

---

promoted (copper-free) azide-alkyne cycloaddition chemistry is highly amenable to on-demand preparation of peptide-PEG-lipids, and the appropriate PEG-lipid precursors are available in a single chemical step from the lipid-PEG-amine building block. Azide-alkyne cycloaddition is especially suitable for disulfide-bridged peptides such as iRGD (cyclic CRGDKGPDC). Added at 10 mol% of a cationic/neutral lipid mixture, the peptide-PEG-lipids stabilize the size of CL–DNA complexes. They also affect cell attachment and uptake of nanoparticles in a peptide-dependent manner, thereby providing a platform for preparing stabilized, affinity-targeted CL–DNA nanoparticles.

Graphical abstract
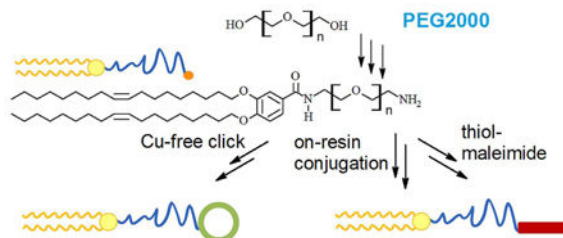
Keywords

Nonviral Gene delivery; Peptide-PEG-lipids; Lipid synthesis; Homing peptides; Nanoparticles; Poly(ethylene glycol); Heterobifunctional poly(ethylene glycol)

Drugs based on nucleic acids (NAs), such as plasmid DNA or short interfering RNA (siRNA), continue to promise a paradigm shift in medicine because they allow the treatment of many diseases at their root cause[1-4]. Much progress [5-7] has been made in the decades since the discovery [8] of efficient, lipid-mediated gene delivery *in vitro*. Investigations of the structures of lipid–NA complexes [9-11], of the barriers to successful transfection that they encounter [12, 13], and of the effect of chemical and physico-chemical properties on their efficiency [14-17] have already yielded highly efficient formulations for *in vitro* applications. However, designing synthetic vectors suitable for *in vivo* applications remains a challenge.

The reason for this are additional requirements, such as stability of the vector in circulation and selectivity for the desired target tissue [18]. Attaching a shell of water-soluble polymer chains to nonviral vectors based on lipids or polymers can stabilize them into nanoparticles. First applied to liposomes [19, 20], this strategy typically uses polyethylene glycol) (PEG) chains of molecular weight 2000 or 5000 g/mol [21]. Unfortunately, the protective PEG covering also interferes with crucial steps in the process of transfection, such as attachment to cells and endosomal escape [22-25]. Current development of nanoparticle vectors is focused on adding functionalities to the PEG coat to offset these drawbacks. Examples include introducing acid-labile bonds that lead to shedding of the PEG shell in the low-pH environment of late endosomes, as well as adding targeting moieties [18, 22, 23, 26, 27].

Peptides are useful targeting moieties because of the vast conformational space they occupy and the ease with which that space can be explored. Techniques such as *in vivo* phage

display [28-30] have led to the discovery of numerous homing peptides for imaging and therapeutic purposes. A variety of tissues can be targeted with appropriate peptides [31, 32], and some peptides even confer additional, therapeutically valuable properties such as cell penetration [33]. Likely the most widely used peptide motif is RGD, the cell adhesion motif from fibronectin [34, 35]. Linear RGD peptides, such as the GRGDSP peptide used in this work, are somewhat promiscuous but bind their integrin receptors ($\alpha_5\beta_1$ integrin is the preferred receptor for GRGDSP) less tightly than cyclic RGD peptides. Conformationally restricted RGD peptides, such as the cyclic c(RGDfK) peptide [36, 37], can selectively target specific integrins such as the $\alpha_v\beta_3$ integrin that is overexpressed in many tumors [38, 39]. The cyclic iRGD (CRGDKGPDC) peptide provides additional benefits: it initially attaches to $\alpha_v\beta_3$ integrin, is then proteolytically cleaved, binds to neuropilin-1, and is internalized [40-42]. Remarkably, it furthermore enables penetration of its cargo into tumor tissue [41, 42] and also inhibits metastasis [43].

Peptides may be attached to lipids to target lipid-based delivery vehicles. To also provide steric stabilization, to inhibit protein-particle interactions, or to maintain targeting ability in the presence of a PEG-lipid without peptide, a spacer of PEG between lipid and peptide is required. Some PEG-lipid building blocks for the synthesis of such peptide-PEG-lipids are commercially available (e.g. from Avanti Polar Lipids), but they are expensive, only provide limited options with regard to conjugation chemistry, and bear saturated tails. The saturated tails may lead to lateral demixing when combined with lipid formulations that achieve high transfection efficiency, because these typically bear unsaturated tails [44,45]

We have synthesized peptide-PEG-lipids using three different approaches. In one of these, the whole molecule was assembled on solid phase support by first assembling the peptide and then coupling a lipid-PEG-carboxylic acid building block to its N-terminus. The other approaches conjugated appropriately functionalized PEG-lipid building blocks and peptides. We employed both the common thiol-maleimide conjugation and a strain-promoted (copper-free) azide-alkyne "click" chemistry (initially developed for the disulfide-bridged iRGD peptide). The details of materials, general and synthesis methods, and characterization techniques are supplied in the Supplementary Material.

The initial approach we pursued to prepare peptide-PEG-lipids is assembly of the complete peptide-PEG-lipid on the solid phase support used for peptide synthesis. Because the PEG-lipid moiety is monofunctional and peptides are built from the C-terminus to the N-terminus in solid phase peptide synthesis, we sought to first assemble the desired peptide and then add the PEG-lipid moiety to its N-terminus. This approach also has the advantage that the required PEG-lipid building blocks could be used on a library of peptide-loaded resins, including ones prepared using automated synthesis. We initially attempted to use the solid support to aid desymmetrization of PEG [46], i.e., to synthesize the PEG-lipid moiety on the resin (by reacting the free N-terminus of the peptide with succinic acid, then coupling with a PEG diamine, and finally attaching our lipid building block 3,4-dioleyloxybenzoic acid (DOB)). This approach was met with limited success (low yields), in particular for longer PEG chains. The likely cause for the low yields, which is crosslinking of two separately anchored moieties on the resin, has been found to reduce yields in attempts at on-resin

cyclization of peptides [47]. Thus, we resorted to preparing a PEG-lipid building block with a distal carboxylic acid (**3**) and coupling this to the protected peptide chain on the resin.

Scheme 1 details the multi-gram scale synthesis of **3**. We prepared PEG-diamine **1** from PEG by two different routes (see Supplementary Material) [48, 49]. Of these, mesylation followed by ammonolysis in a large excess of ammonium hydroxide solution [49] proved much preferable. Desymmetrization of **1** to yield the lipid-PEG-amine **2** is a key step in all our approaches to peptide-PEG-lipids. Low temperature and an only moderately reactive acylation agent (the pentafluorophenyl ester of DOB) were essential to prevent excessive, undesired diacylation [50] of the PEG diamine with DOB. We then separated the obtained mixture of **2** and undesired symmetric PEG-derivatives (DOB-PEG-DOB and PEG diamine) by dry column vacuum chromatography [51]. This separation is aided by the strong effect that both the DOB-moiety and the amine endgroup have on the elution behaviour of PEG, even at long chain lengths. Reaction with succinic acid anhydride readily converted the amine endgroup of PEG-lipid **1** into a carboxylic acid to give **3**. We then coupled this building block to the peptide on the resin and performed the deprotection and cleavage from the resin by standard peptide synthesis methods to obtain the desired peptide-PEG-lipid (Scheme 2).

While conceptually straightforward and amenable to gram-scale synthesis, the direct solid phase synthesis approach shown in Scheme 2 is less suitable for cyclic peptides and separately prepared libraries of purified peptides. Thus, we also explored alternative synthesis routes to peptide-PEG-lipids. These approaches conjugate deprotected, purified and appropriately functionalized peptides with matching PEG-lipid building blocks. The choices for conjugation chemistries are limited by the variety of reactive functional groups on peptide sidechains, but several options exist. One of the most commonly employed peptide conjugation methods is the maleimide-thiol conjugation. We employed this method in the preparation of a peptide-PEG-lipid bearing the RPARPAR sequence. The RPARPAR peptide, displaying a prototypical CendR motif [40], binds to neuropilin-1, which mediates cellular internalization and tissue penetration [40]. As shown in Scheme 3, we prepared a maleimide-functionalized PEG-lipid **4** from the amine-functionalized PEG-lipid **2** by acylation with the commercially available bifunctional linker EMCA (6-maleimidohexanoic acid).

Thiol-functionalization of RPARPAR is straightforward because this peptide does not contain thiol groups or disulfide bridges. This, however, is not the case for the iRGD peptide, which contains a disulfide bond. Preparation of thiol-functionalized disulfide-containing peptides is problematic because the resulting peptides are prone to cleavage or scrambling of the disulfide bonds due to the presence of the free thiol group. However, disulfide bonds are a convenient way to induce conformational restraints on a peptide chain. Thus, we sought to develop an alternative conjugation method that is compatible with disulfide-containing peptides such as iRGD.

Biorthogonal chemistry has provided a collection of conjugation methods that are compatible with the wide variety of chemical functional groups on biological molecules and in biological environments [52, 53]. A recent implementation of the strain-promoted, copper-free, azide-alkyne dipolar (Huisgen) cycloaddition stood out because it provides facile

access to a strained cyclic alkyne building block that can be conjugated to amine groups [54]. Thus, we prepared bicyclononyne-functionalized PEG-lipid **5** (Scheme 3) from the amine-functionalized PEG-lipid **2**. The cycloaddition conjugation of this building block with azide-functionalized peptides in acetonitrile/water (3:1, v:v) proceeded smoothly. We used this method to prepare PEG-lipids with distally attached cyclic iRGD peptide (CRGDKGPDC) [40-42].

To determine the effect of peptide-PEG-lipids on the steric stabilization and charge of CL–DNA complexes, we measured the size (using dynamic light scattering) and ζ-potential of the complexes. As a control PEG-lipid without peptide, we used DOB-mPEG2000, the ester of DOB with monomethoxy-PEG2000. (See the Supplementary Material for structure and synthesis.) Table 1 compiles the results of measurements performed on complexes at a lipid/DNA charge ratio (ρ) of 5, prepared from an MVL5[55,56]/DOPC/(peptide-)PEG-lipid lipid mixture (10/80/10 molar ratio). The size measurements were performed both in water and the cell culture medium (DMEM: Dulbecco's modified Eagle's medium). Electrostatic repulsion can stabilize small particles even for complexes without PEGylation in water, but the salt in DMEM screens this repulsion and thereby leads to aggregation of complexes that are not sterically stabilized [22]. As evident from Table 1, the peptide-PEG-lipids effectively stabilize CL–DNA complexes into nanoparticles with a diameter of about 100 nm. The size of most of these nanoparticles is larger in DMEM than in water, but the difference is small; CL–DNA complexes lacking steric stabilization form micrometer-size aggregates in DMEM [22]. The ζ-potential of all CL–DNA nanoparticles is positive, with that of particles formed with the DOB-mPEG2000 lipid (without peptide) and the RPARPAR-PEG2K-lipid being particularly high. A possible explanation [23] is that the added size of the peptides (with a molecular weight of $\approx$600 to 1000 Da) expands the PEG corona, thereby decreasing the ζ-potential which is measured at the slipping plane between particle and solution. For the RPARPAR-PEG2K-lipid, this effect may be offset by the positive charge ($+2e$) of the peptide.

To assess whether peptide ligands attached to PEG-lipids improve attachment of CL–DNA nanoparticles to cells and promote their uptake, we used flow cytometry and optical microscopy with fluorescently labeled nanoparticles. As a model human cancer cell line, we used PC-3 (prostate cancer) cells. We performed these measurements with nanoparticles prepared from the same lipid mixtures used in the DLS studies (MVL5/DOPC/ (peptide-)PEG-lipid at 10/80/10 molar ratio), i.e., at relatively low membrane charge density (σ_M). We have previously shown (for nanoparticles based on the monovalent cationic lipid DOTAP (2,3-dioleyloxypropyltrimethylammonium chloride)) that low σ_M reduces the nonspecific electrostatic attraction between negatively charged cell membranes and positively charged nanoparticles [23].

In Figure 1, panels A and B show flow cytometry data for nanoparticles prepared with the different (peptide-)PEG-lipids and fluorescently labeled DNA as well as controls. For the data in Figure 1A, the cells were washed with PBS and suspended in DMEM prior to analysis. Thus, nanoparticles that do not adhere strongly to cells or have been internalized are washed off and not detected. For the data in Figure 1B, Trypan Blue dye was added to the cells after the washing steps. This quenches the fluorescence of all material accessible to

the dye, i.e., outside of the cells [57]. In this way, it is possible to distinguish between tightly bound and internalized particles, a distinction often missing in the literature.

Particles prepared with the linear RGD-PEG-lipid (pink curves in Fig. 1(A,B)) show the largest amount of cell attachment, but also the largest reduction in signal when Trypan Blue is added. In contrast, particles containing PEG-lipid without peptide ligand (blue curves) show the weakest attachment, but also the smallest shift upon quenching of outside particles. This is likely due to the fact that they bind to cells weakly enough to be washed off almost completely. The effect of quenching is similarly small for RPARPAR-tagged particles, suggesting that they either also bind only weakly or, more likely, that they internalize quickly and efficiently. The fluorescence intensity of cells treated with these particles (with and without Trypan Blue) is higher than of cells treated with particles without peptide, demonstrating the effect of the RPARPAR ligand. Tagging particles with iRGD peptides (orange curves) also increases their attachment to cells. However, treatment with Trypan Blue strongly reduces fluorescence to below the level of particles without ligands.

Plotting mean fluorescence intensity for both flow cytometry measurements (Figure 1C) summarizes key aspects of the data. Here, the height of the lighter bars represents the mean in the presence of Trypan Blue while the height of the darker bars represents the mean without Trypan Blue treatment. As mentioned, the linear RGD peptide leads to a very high level of binding of nanoparticles to cells. Because the investigated peptides bind to different receptors on the cell surface, this does not reflect their relative binding affinity but rather a combination of binding affinity and receptor density on the cell. Another interesting feature of the data is the large difference between attached and internalized particles for the RGD-type peptides compared to RPARPAR and unfunctionalized particles. Further investigations are underway to determine whether this is simply due to a very high binding affinity of RGD-based peptides or because these particles might undergo not only binding and internalization but also recycling to the cell surface.

Figure 2 shows optical micrographs of live cells incubated with fluorescently labeled CL–DNA nanoparticles with and without peptide ligands. The images confirm the findings from flow cytometry regarding the amount of particle attachment and uptake. They also reveal that the intracellular distribution of particles differs. The majority of both RPARPAR-tagged and untagged particles are localized in the perinuclear region. In contrast, the distribution of particles tagged with RGD-type peptides inside the cell is more diffuse. This likely reflects different pathways of internalization or intracellular processing, which thus can be selected by choosing the appropriate peptide-PEG-lipid. For reference, imaging results for cells incubated with labeled DNA only are shown in Figure S1 in the Supplementary Material.

Optical imaging also yields further information that may explain the surprisingly low uptake for iRGD-tagged nanoparticles. Incubation with these particles results in a large number of cells detaching from the surface and aggregating (see Figure S2 in the Supplementary Material). These cells, which presumably have bound comparatively large numbers of nanoparticles, are lost in the washing steps of the flow cytometry protocol and are thus not counted in these measurements. It is interesting to speculate that this property of iRGD-

tagged particles may be related to the ability of iRGD to penetrate deep into tumor tissue *in vivo*.

Efficient, selective CL–DNA vectors for *in vivo* applications will have to incorporate targeting and other functional moieties. We have described and compared three methods of preparing peptide-PEG-lipids and demonstrated the use of these molecules in stabilizing CL–DNA complexes into nanoparticles, targeting the particles to cells, and facilitating their internalization. PEG desymmetrization and peptide conjugation are the key steps in a general approach for the synthesis of peptide-PEG-lipids. The methods we have described will facilitate access to this useful class of compounds, a foundation for further exploration of the effect of chemical structure, e.g., of lipid tail and linker. Synthesis of the peptide-PEG-lipids on a solid support using a PEG-lipid carboxylic acid is most useful for larger scale synthesis and simple peptides, whereas the conjugation methods are best suited for on-demand preparation of peptide-PEG-lipids from peptides obtained commercially or prepared by automated synthesis. Conjugation using strain-promoted azide–alkyne cycloaddition avoids complications with thiol oxidation or disulfide scrambling that can plague thiol-maleimide conjugations. Tagging of CL–DNA nanoparticles with peptide ligands promotes their attachment to cells and, for the linear RGD and the RPARPAR peptides, also their internalization. While we have used peptides as model ligands in this work, the developed synthesis strategy (in particular the PEG desymmetrization) can readily be applied to other small molecule ligands, and the thiol-maleimide conjugation can be used to couple antibody fragments and aptamers.

Supplementary Material

Refer to Web version on PubMed Central for supplementary material.

Acknowledgments

References

1. Sheridan C. Nat Biotechnol. 2012; 30:471. [PubMed: 22678364]

2. Davis ME. Mol Pharmaceutics. 2009; 6:659.

3. Ginn SL, Alexander IE, Edelstein ML, Abedi MR, Wixon J. J Gene Med. 2013; 15:65. [PubMed: 23355455]

4. Yin H, Kanasty RL, Eltoukhy AA, Vegas AJ, Dorkin JR, Anderson DG. Nat Rev Genet. 2014; 15:541. [PubMed: 25022906]

5. Huang, L.; Liu, D.; Wagner, E. Nonviral Vectors for Gene Therapy: Lipid- and Polymer-based Gene Transfer. Academic Press; New York: 2014. Eds.

6. Huang, L.; Hung, MC.; Wagner, E. Non-Viral Vectors for Gene Therapy. Academic Press; New York: 2005. Eds.

7. Huang, L.; Hung, MC.; Wagner, E. Nonviral Vectors for Gene Therapy. Academic Press; San Diego: 1999. Eds.

8. Felgner PL, Gadek TR, Holm M, Roman R, Chan HW, Wenz M, Northrop JP, Ringold GM, Danielsen M. Proc Natl Acad Sci U S A. 1987; 84:7413.

9. Safinya CR, Ewert KK, Leal C. Liq Cryst. 2011; 38:1715.

10. Majzoub RN, Ewert KK, Jacovetty EL, Carragher B, Potter CS, Li Y, Safinya CR. Langmuir. 2015; 31:7073. [PubMed: 26048043]

11. Silva BFB, Majzoub RN, Chan CL, Li Y, Olsson U, Safinya CR. Biochim Biophys Acta, Biomembr. 2014; 1838:398.

12. Zuhorn I, Engberts J, Hoekstra D. Eur Biophys J. 2007; 36:349. [PubMed: 17019592]

13. Ewert KK, Zidovska A, Ahmad A, Bouxsein NF, Evans HM, McAllister CS, Samuel CE, Safinya CR. Top Curr Chem. 2010; 296:191. [PubMed: 21504103]

14. Safinya CR, Ewert KK, Majzoub RN, Leal C. New J Chem. 2014; 38:5164.

15. Chan CL, Ewert KK, Majzoub RN, Hwu YK, Liang KS, Leal C, Safinya CR. J Gene Med. 2014; 16:84. [PubMed: 24753287]

16. Tranchant I, Thompson B, Nicolazzi C, Mignet N, Scherman D. J Gene Med. 2004; 6:S24. [PubMed: 14978748]

17. Middaugh CR, Ramsey JD. Anal Chem. 2007; 79:7240. [PubMed: 17972398]

18. Lin G, Zhang H, Huang L Mol. Pharmaceutics. 2015; 12:314.

19. Gabizon A, Papahadjopoulos D. Proc Natl Acad Sci U S A. 1988; 85:6949.

20. Allen TM, Hansen C, Rutledge J. Biochim Biophys Acta, Biomembr. 1989; 981:27.

21. Lasic DD, Needham D. Chem Rev. 2002; 95:2601.

22. Chan CL, Majzoub RN, Shirazi RS, Ewert KK, Chen YJ, Liang KS, Safinya CR. Biomaterials. 2012; 33:4928. [PubMed: 22469293]

23. Majzoub RN, Chan CL, Ewert KK, Silva BFB, Liang KS, Jacovetty EL, Carragher B, Potter CS, Safinya CR. Biomaterials. 2014; 35:4996. [PubMed: 24661552]

24. Martin-Herranz A, Ahmad A, Evans HM, Ewert K, Schulze U, Safinya CR. Biophys J. 2004; 86:1160. [PubMed: 14747350]

25. Majzoub RN, Chan CL, Ewert KK, Silva BFB, Liang KS, Safinya CR. Biochim Biophys Acta, Biomembr. 2015; 1848:1308.

26. Torchilin VP. Nat Rev Drug Discovery. 2014; 13:813. [PubMed: 25287120]

27. Walker GF, Fella C, Pelisek J, Fahrmeir J, Boeckle S, Ogris M, Wagner E. Mol Ther. 2005; 11:418. [PubMed: 15727938]

28. Pasqualini R, Ruoslahti E. Nature. 1996; 380:364. [PubMed: 8598934]

29. Bábí(x0010D)ková J, Tóthová (x0013D), Boor P, Celec P. Biotechnol Adv. 2013; 31:1247. [PubMed: 23623852]

30. Teesalu, T.; Sugahara, KN.; Ruoslahti, E. Methods in Enzymology. Wittrup, KD.; Gregory, LV., editors. Vol. 503. Academic Press; San Diego: 2012. p. 35-56.

31. Ruoslahti E, Rajotte D. Annu Rev Immunol. 2000; 18:813. [PubMed: 10837076]

32. Ruoslahti E. Biochem Soc Trans. 2004; 32:397. [PubMed: 15157146]

33. Ruoslahti E, Duza T, Zhang L. Curr Pharm Des. 2005; 11:3655. [PubMed: 16305501]

34. Pierschbacher MD, Ruoslahti E. Nature. 1984; 309:30. [PubMed: 6325925]

35. Ruoslahti E, Pierschbacher MD. Cell. 1986; 44:517. [PubMed: 2418980]

36. Gurrath M, Müller G, Kessler H, Aumailley M, Timpl R. Eur J Biochem. 1992; 210:911. [PubMed: 1483474]

37. Kessler H, Diefenbach B, Finsinger D, Geyer A, Gurrath M, Goodman SL, Hölzemann G, Haubner R, Jonczyk A, Müller G, Roedern EG, Wermuth J. Lett Pept Sci. 1995; 2:155.

38. Meyer A, Auernheimer J, Modlinger A, Kessler H. Curr Pharm Des. 2006; 12:2723. [PubMed: 16918408]

39. Ruoslahti E, Bhatia SN, Sailor MJ. J Cell Biol. 2010; 188:759. [PubMed: 20231381]

40. Teesalu T, Sugahara KN, Kotamraju VR, Ruoslahti E. Proc Natl Acad Sci U S A. 2009; 106:16157.

41. Sugahara KN, Teesalu T, Karmali PP, Kotamraju VR, Agemy L, Girard OM, Hanahan D, Mattrey RF, Ruoslahti E. Cancer Cell. 2009; 16:510. [PubMed: 19962669]

42. Sugahara KN, Teesalu T, Karmali PP, Kotamraju VR, Agemy L, Greenwald DR, Ruoslahti E. Science. 2010; 328:1031. [PubMed: 20378772]

43. Sugahara KN, Braun GB, de Mendoza TH, Kotamraju VR, French RP, Lowy AM, Teesalu T, Ruoslahti E. Mol Cancer Ther. 2015; 14:120. [PubMed: 25392370]

44. Heyes J, Palmer L, Bremner K, MacLachlan I. J Controlled Release. 2005; 107:276.

45. Koynova R, Tenchov B, Wang L, MacDonald RC. Mol Pharmaceutics. 2009; 6:951.

46. Bettinger T, Remy JS, Erbacher P, Behr JP. Bioconjugate Chem. 1998; 9:842.

47. Kessler H. personal communication.

48. Zalipsky S, Gilon C, Zilkha A. Eur Polym J. 1983; 19:1177.

49. Aronov O, Horowitz AT, Gabizon A, Gibson D. Bioconjugate Chem. 2003; 14:563.

50. Jacobson AR, Makris AN, Sayre LM. J Org Chem. 1987; 52:2592.

51. Pedersen DS, Rosenbohm C. Synthesis. 2001:2431.

52. Bertozzi CR. Acc Chem Res. 2011; 44:651. [PubMed: 21928847]

53. Debets MF, van Berkel SS, Dommerholt J, Dirks AJ, Rutjes FPJT, van Delft FL. Acc Chem Res. 2011; 44:805. [PubMed: 21766804]

54. Dommerholt J, Schmidt S, Temming R, Hendriks LJA, Rutjes FPJT, van Hest JCM, Lefeber DJ, Friedl P, van Delft FL. Angew Chem, Int Edit Engl. 2010; 49:9422.

55. Ewert K, Ahmad A, Evans HM, Schmidt HW, Safinya CR. J Med Chem. 2002; 45:5023. [PubMed: 12408712]

56. Ahmad A, Evans HM, Ewert K, George CX, Samuel CE, Safinya CR. J Gene Med. 2005; 7:739. [PubMed: 15685706]

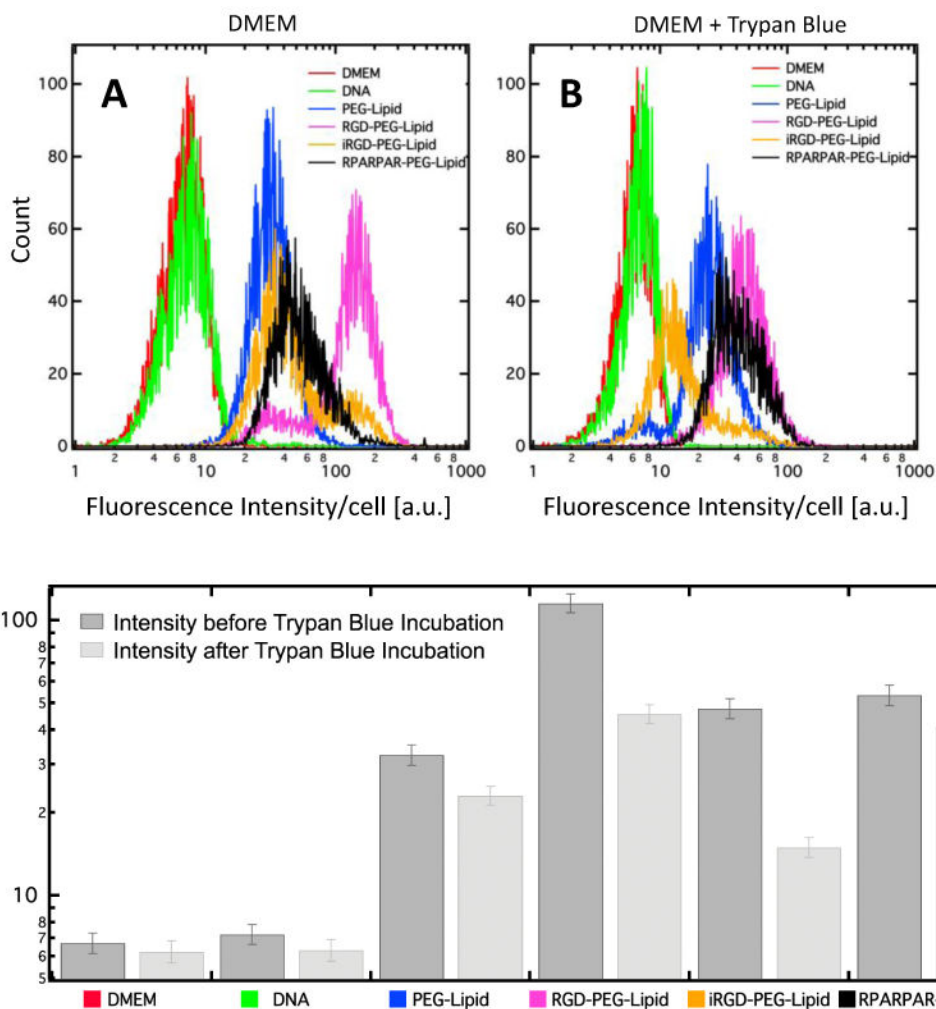57. Bjerknes R, Bassøe CF. Blut. 1984; 49:315. [PubMed: 6435701]

Figure 1.

Flow cytometry measurements of attachment and uptake of CL–DNA nanoparticles. PC-3 cells were incubated with DMEM medium, labeled DNA (10% (w/w) of DNA labeled with YOYO-1), or nanoparticles containing labeled DNA. The nanoparticles were formulated at $\rho=5$ with lipid mixtures of MVL5/DOPC/(peptide-)PEG-lipid (10/80/10, mol/mol/mol). (A) Data for cells incubated with nanoparticles for 5 h. (B) Data for cells incubated with nanoparticles for 5 h and subsequently exposed to Trypan Blue to quench extracellular fluorescence. (C) Plot of mean fluorescence intensities for the data in parts A and B. The height of the dark bars represents the geometric mean of cells that were incubated with nanoparticles for 5 hours (part A), while the height of the lighter bars indicates the geometric mean of the same samples in the presence of Trypan Blue (part B). For all investigated peptides, peptide-tagging of nanoparticles improves binding over the control (PEG-lipid without peptide). Peptide-tagging also improves internalization except in the case of the iRGD-PEG2K-lipid.
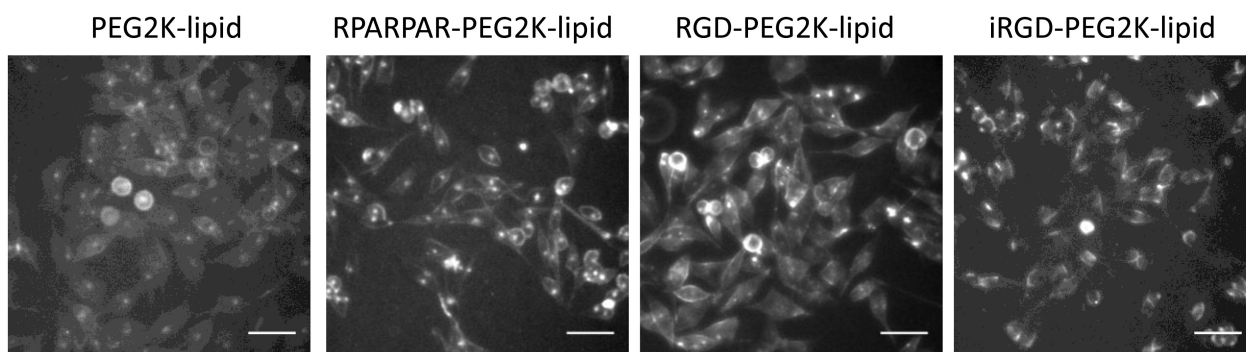
| PEG2K-lipid | RPARPAR-PEG2K-lipid | RGD-PEG2K-lipid | iRGD-PEG2K-lipid |

Figure 2.
Live cell imaging of the interaction of PEGylated CL–DNA nanoparticles with and without targeting peptides with PC-3 cells. Cells were incubated with nanoparticles for 5 h before imaging. CL–DNA nanoparticles were formulated with fluorescently-labeled plasmid DNA (15% (w/w) of DNA labeled with YOYO-1) at $\rho=5$ with lipid mixtures of MVL5/DOPC/(peptide-)PEG-lipid (10/80/10 molar ratio). All scale bars are 50 µm.
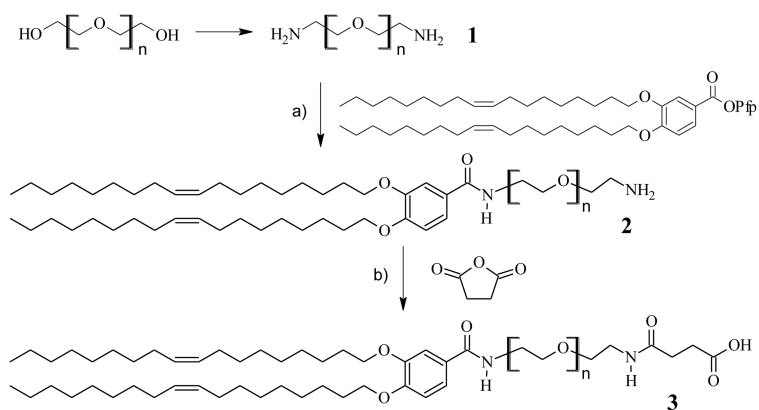
Scheme 1.
Synthesis of amine- and carboxylic acid-functionalized PEG-lipids; n≈45 (PEG MW=2000 g/mol). a) −78 °C to room temperature; b) DIEA, room temperature; DIEA: *N,N*-diisopropylethylamine; HOPfp: pentafluorophenol.
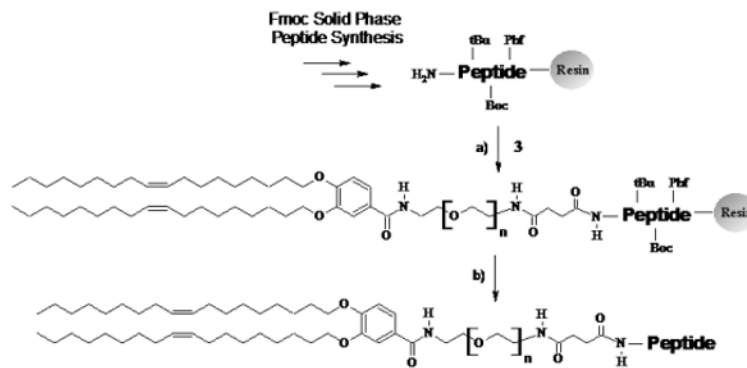
Scheme 2.
Solid phase synthesis of peptide-PEG-lipids. a) TBTU, HOBt, DIEA; b) 1% TFA in dichloromethane, then 95% TFA in water (for GRGDSP peptide); DIEA: *N,N*-diisopropylethylamine; HOBt: 1-hydroxybenzotriazole hydrate; TBTU: O-benzotriazol-1-yl-*N,N,N′,N′*-tetramethyluronium tetrafluoroborate; TFA: trifluoroacetic acid.
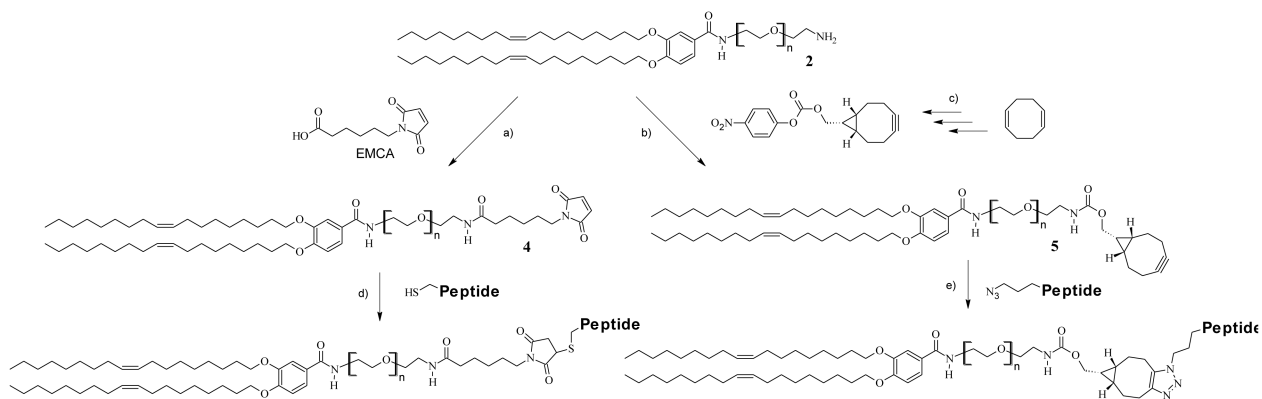
Scheme 3.
Synthesis of peptide-PEG-lipids by conjugation with free peptides. a) TBTU, DIEA; b) Et$_3$N; c) reference 49; d) MeCN/PBS (1:1, v:v), nitrogen atmosphere; e) MeCN/water (3:1, v:v); DIEA: *N*,*N*-diisopropylethylamine; PBS: phosphate-buffered saline; TBTU: O-benzotriazol-1-yl-*N*,*N*,*N*′,*N*′-tetramethyluronium tetrafluoroborate.

Table 1

Size and ζ-potential of CL–DNA complexes prepared at ρ=5 from an MVL5/DOPC/(peptide-)PEG-lipid lipid mixture (10/80/10 molar ratio). The listed values are the mean of two measurements ± SD.

	Hydrodynamic diameter in water [nm]	Hydrodynamic diameter in DMEM [nm]	ζ-potential [mV]
DOB-mPEG2000	108.5 ± 2.3	105.8 ± 1.6	47.6 ± 2.5
RGD-PEG2K-lipid	86.5 ± 2.1	117.1 ± 0.7	32.8 ± 0.3
iRGD-PEG2K-lipid	117.6 ± 1.9	107.7 ± 0.1	34.9 ± 0.3
RPARPAR-PEG2K-lipid	96.62 ± 5.38	139.3 ± 2.3	47.5 ± 4.5